



**HAL**  
open science

## Decomposition of $\beta$ -metastable phase in $\beta$ -Cez alloy during continuous heating

R. Sanguinetti, M. Zandona, A. Pianelli, E. Gautier

► **To cite this version:**

R. Sanguinetti, M. Zandona, A. Pianelli, E. Gautier. Decomposition of  $\beta$ -metastable phase in  $\beta$ -Cez alloy during continuous heating. *Journal de Physique IV Proceedings*, 1993, 03 (C7), pp.C7-527-C7-531. 10.1051/jp4:1993785 . jpa-00252205

**HAL Id: jpa-00252205**

**<https://hal.science/jpa-00252205>**

Submitted on 4 Feb 2008

**HAL** is a multi-disciplinary open access archive for the deposit and dissemination of scientific research documents, whether they are published or not. The documents may come from teaching and research institutions in France or abroad, or from public or private research centers.

L'archive ouverte pluridisciplinaire **HAL**, est destinée au dépôt et à la diffusion de documents scientifiques de niveau recherche, publiés ou non, émanant des établissements d'enseignement et de recherche français ou étrangers, des laboratoires publics ou privés.

## Decomposition of $\beta$ -metastable phase in $\beta$ -Cez alloy during continuous heating

R. SANGUINETTI, M. ZANDONA, A. PLANELLI and E. GAUTIER

*Laboratoire de Science et Génie des Matériaux Métalliques, URA 159 du CNRS, Ecole des Mines, Parc de Saurupt, 54042 Nancy cedex, France*

### Abstract

The decomposition of the metastable  $\beta$  phase in  $\beta$  Cez alloy has been studied during continuous heating up to 830°C. The heating rate varied between 0.25 and 5°C/s. Electric resistivity measurements, and hardness measurements revealed different phase transformations as temperature increased. Different samples were quenched from different temperatures during the heating range and were then studied by X-ray and TEM, allowing to correlate the changes in resistivity measurements to the beginning of the precipitations of the  $\omega$  and  $\alpha$  phases and to establish the continuous heating transformation diagram. A change in the resistivity variations, not dependent on the heating rate was observed near 700°C. X-ray quantitative analysis and EAM studies revealed that the structure consisted of a maximal content of  $\alpha$  phase, surrounded by  $\beta$  rich zones in the matrix. For temperatures greater than 700°C, the content of  $\alpha$  phase diminished and the  $\beta$  phase was homogenized.

### Introduction

The  $\beta$  metastable decomposition during continuous heating is of considerable importance since it determines the morphology and distribution of the  $\alpha$  precipitates during ageing treatments in the  $\alpha + \beta$  domains.

For the pseudo  $\beta$  titanium alloy, the optimal microstructure is obtained by a sequence of thermomechanical and thermal treatments. Also the final microstructure is highly dependent on the various parameters of these treatments.

Also we investigated the effects of the cooling rate from the  $\beta$  range solution treatment to room temperature on the further phase transformations, during a further solution treatment in the  $\alpha + \beta$  temperature range.

In this paper we focus on the phase transformations occurring during heating, the initial structure being a  $\beta$  metastable phase obtained by quenching after a solution treatment in the  $\beta$  phase. The effect of the cooling rate from the  $\beta$  solution treatment on the microstructure is presented elsewhere (1).

## Experimental methods

The alloy used in this study was a "pseudo-beta" alloy named  $\beta$ -Cez which was produced by Cezus. The nominal composition in weight percent of the as-received material was Ti-5Al-2Sn-4Zr-4Mo-2Cr-1Fe and the dimensions of the cylindrical samples were  $D = 6.0$  mm and  $L = 25.0$  mm;

Specimens were solution treated in secondary vacuum at  $920^\circ$  for 30 min. and were then water-quenched. The specimens were then reheated up to  $830^\circ\text{C}$  at different rates, while changes in electrical resistivity were recorded. Moreover, specimens were helium quenched from different temperatures in the heating range in order to study the phases in presence by X-ray and TEM. All X-ray bulk samples were cutted and then mechanically polished. A cobalt anticathod ( $\text{Co} - \text{K} \alpha_1$ ;  $\lambda = 1.7889 \text{ \AA}$ ) was used to obtain the X-ray diffraction patterns. Thin foils were prepared by Blackburn-Williams (2) solution with the Bainbridge-Thorne (3) Jet polish technique, for investigations by TEM and AEM.

Hardness measurements were made too on the bulk samples, using the Hv30 standard measurements test.

## Results

### a - Electrical resistivity

The electrical resistivity variation curves were recorded versus time and temperature. Slope changes were observed at different temperatures which depended on the heating rate as shown figure 1. Four domains can be considered of which limit temperatures versus heating rate are given in table 1. A slope change not dependent on the heating rate, was observed near  $700^\circ\text{C}$ .

Domains	Heating rates Temperature	$0.25^\circ\text{C/s}$	$0.50^\circ\text{C/s}$	$1.25^\circ\text{C/s}$	$5.0^\circ\text{C/s}$
1	$20^\circ\text{C}$ up to $T_1$	$300^\circ\text{C}$	$300^\circ\text{C}$	$350^\circ\text{C}$	$450^\circ\text{C}$
2	$T_1$ up to $T_2 =$	$350^\circ\text{C}$	$350^\circ\text{C}$	$400^\circ\text{C}$	$550^\circ\text{C}$
3	$T_2$ up to $T_3 =$	$700^\circ\text{C}$	$700^\circ\text{C}$	$700^\circ\text{C}$	$700^\circ\text{C}$
4	$T_3$ up to $T_4 =$	$830^\circ\text{C}$	$830^\circ\text{C}$	$830^\circ\text{C}$	$830^\circ\text{C}$

Table 1 - Limit temperatures of the domains for different heating rates

### b - Hardness measurements

The variations of hardness of the samples obtained after quenching from the different temperatures are shown figure 2 for a rate of  $0.5^\circ\text{C/s}$ . No significant increase in hardness is observed in the first domain ; an increase in hardness is noticed in the second and third domains. At quench temperatures greater than  $700^\circ\text{C}$ , the hardness fellled down, and was nearly constant after 60 min at  $830^\circ\text{C}$ . A maximal hardness value was observed near  $700^\circ\text{C}$ , for all heating rates used.

### c - Microstructure

X-ray measurement of the initial  $\beta$  water quenched phase revealed that the structure consisted of beta metastable phase with anisothermal  $\omega$  phase. Electron diffraction patterns taken from the beta-metastable structure in the first domain revealed weak and diffusional streaks, which later could be observed too and identified by X-ray as being the athermal omega phase. This phase is produced by rapid quenching after solution treatment and vanishes at the

end of this domain. It was difficult to discern the shapes in that scattering dark shades. On the morphological point of view it looks like the G.P. zones found in the Al-Zn-Mg systems (4-7).

Specimens quenched from a temperature in the second domain revealed changes in contrast when observing the matrix. EDAX analysis showed that the transformed matrix has a light heterogeneousness of the composition and so we called it as beta transient ( $\beta_T$ ). Electron diffraction patterns taken from  $\beta_T$  revealed peaks of the isothermal omega phase (fig. 3). However, that phase which was always associated with  $\beta_T$  could not be observed in dark field conditions. Lattice parameters of the hexagonal  $\omega$  athermal or isothermal phases have been found as  $a = 4.53 \text{ \AA}$  and  $c = 2.78 \text{ \AA}$ . The Silcock orientation relationships  $\langle 111 \rangle_\beta // \langle 0001 \rangle_\omega$  and  $\{110\}_\beta // \{11\bar{2}0\}_\omega$  were obtained. The isothermal  $\omega$  phase vanished on the initial stages of the third domain during continuous heating, while alpha phase was beginning to precipitate.

Selected area diffraction patterns taken from regions around alpha precipitates in the third domain showed splitting and diffuse spots. The only observable feature of the electron diffraction pattern, apart from the diffuse streaking, was the splitting of the matrix spots.

X-Ray diffractograms and TEM electron diffraction patterns showed that the structure consisted of the h.c.  $\alpha$  phase and the b.c.c.  $\beta$  phase; EDAX analysis revealed that the composition of the  $\alpha$  precipitates is roughly constant, however that of the  $\beta$  phase is enriched in Fe, Cr and Mo around the  $\alpha$  phase.

The variations in chemical composition of the zones around the  $\alpha$  phase lead to a decrease in the "d spacing" resulting to the splitting of the matrix spots. These zones are called rich beta phase ( $\beta_r$ ). It was observed that the nucleation of the alpha phase within a grain occurs near the interfaces between the  $\beta_r$  and the matrix which we thought to be ex-omega. This result is in agreement with Narayanan and Archbold (8), Campagnac and Vassel (9).

In the fourth domain, we observed a reduction of the  $\alpha$  lamellae density followed by its coalescence. While the  $\alpha$  phase content diminished, at temperatures greater than  $700^\circ\text{C}$  the composition of the  $\beta$  rich zones and the matrix was homogenized to form an equilibrium beta phase. The B $\ddot{u}$ rgers orientation relationships  $\langle 111 \rangle_\beta // \langle 11\bar{2}0 \rangle_\alpha$  and  $\{110\}_\beta // \{0001\}_\alpha$  were obtained when the temperature reached about  $830^\circ\text{C}$  (Fig. 4).

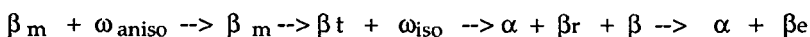
#### d - X-Ray

X-ray diffraction patterns were obtained for the as quenched samples to determine the structure parameters in the present phases and to estimate the content of the  $\alpha$  phase. The ratio  $I_\alpha / (I_\alpha + I_\beta)$  (fig. 5) shows an indication on the  $\alpha$  phase content variations versus the temperature for a heating rate of  $0.5^\circ\text{C/s}$ ; where  $I_\alpha$  and  $I_\beta$  are the sum of peak intensities of the  $\alpha$  and  $\beta$  phases respectively.

The ratio  $I_\alpha / (I_\alpha + I_\beta)$  increases up to  $700^\circ\text{C}$ , indicating a maximal content of alpha phase. For temperatures higher than  $700^\circ\text{C}$  this ratio falls down to establish near  $830^\circ\text{C}$ .

## Discussion

Changes in electrical resistivity as in hardness measurements observed during continuous heating revealed the occurrence of different phase transformations. The T.E.M. and X.R. studies allowed to define that the decomposition of the metastable beta phase of the beta Cez alloy during continuous heating consisted of a sequence of successive phase transformations:



were  $\beta_m$ ,  $\beta_t$ ,  $\beta_r$ ,  $\beta$  and  $\beta_e$  refer to the metastable, transient, enriched, matrix and equilibrium  $\beta$  phases respectively.

At temperatures below  $T_2$  [350 to 550°C, depending on the heating rate], the different observations indicate that the decomposition of the metastable  $\beta$  phase into  $\omega$  phase could proceed through a diffusional clustering mechanism. Such a result has been pointed out by Narayanan and Archbold on Ti-13V-11Cr-3Al previously (8).

At temperatures above  $T_2$ , the precipitation occurs. The chemical composition of the  $\beta$  phase is heterogeneous,  $\beta$  zones enriched in Cr, Fe and Mo surrounded the  $\alpha$  lamellae. A maximal content of  $\alpha$  phase not dependent on the heating rate is obtained near 700°C as shown by X-ray intensity ratio variations as by a maximum in the hardness measurements.

Selected area diffraction patterns and EDAX analysis suggest that the precipitation could occur through composition fluctuations in the matrix leading to the formation of solute rich zones which subsequently drive to a maximal content of the alpha phase.

Therefore, it is reasonable to believe that the metastable  $\beta$  phase decomposition mechanism is dependent on the matrix composition fluctuation, during continuous heating. The fluctuations can be related to a diffusional vacancy mechanism as suggested by different authors (4-8).

### Acknowledgments

This work was realized in the frame of "GDR" Relations Structures/Propriétés des alliages de titane transformés à partir du domaine beta" supported by CNRS, DRET - DGA, AEROSPATIALE, AUBERT ET DUVAL, CEZUS, FORTECH DIVISION AIRFORGE PAMIERS, SEP, SNECMA and TURBOMECA.

### References

- [1] - SANGUINETTI R. , GAUTIER E. , PIANELLI A. and ZANDONA M. , PROC. 36ème Colloque de Métallurgie, to be published; Journal de Physique.
- [2] - BLACKBURN M.J. and WILLIAMS J.C.- Trans. AIME, vol. 239, 1967, 287.
- [3] - BAINBRIDGE J.E. and THORNE L. - Journal Nucl. Mat. vol. 34, 1970, 202.
- [4] - CASTAING R. - Revue de Métallurgie, vol. 52, n° 9, 1955, 669-675.
- [5] - NEWKIRK J.B. - A.S.T.M. Ohio USA 1957, 6-349.
- [6] - ARCHAMBAULT P. - Thèse d'Etat INPL Nancy; 7 Février 1985.
- [7] - EMBURY J.D. and NICHOLSON R.B. - Acta Metallurgica, vol 13, april 1965, 403-417
- [8] - NARAYANAN G.H. and ARCHBOLD T.F. - Metallurgical Transactions Vol. 1, August 1970 ; 2281 - 2290..
- [9] - CAMPAGNAC M.H. and VASSEL A. - Sixth world conference on Titanium - France 1988, 1619 - 1624. Ed. by Lacombe, Tricot and Béganger.

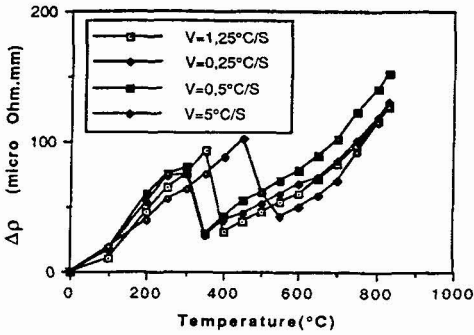


Fig. 1 - Electrical resistivity variations versus temperature during heating up to 830°C for different heating rates

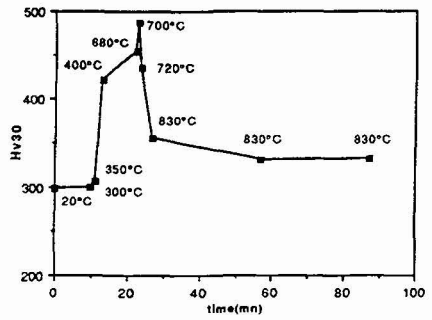


Fig. 2 - Hardness measurement variations for specimens cooled at different times (or temperatures) during heating (heating rate 0.5°C).

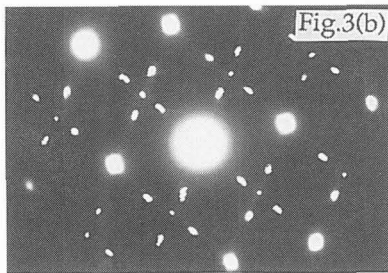
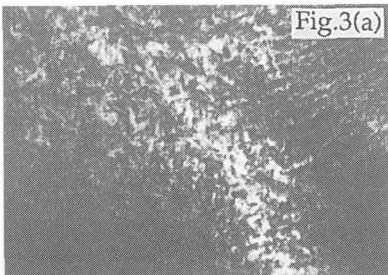


Fig. 3 - (a) Dark field image taken from the second domain showing a transformed beta transient matrix ( $\beta_t$ )  $T=350^\circ\text{C}$ . (b) The  $\omega$  phase was observed in SAD pattern, although this phase was not observed in dark field image. Magnification 100000X.

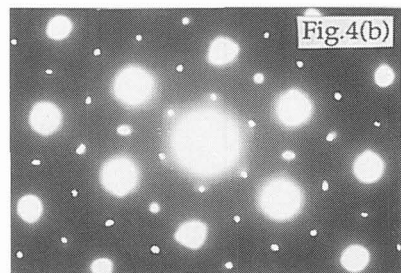
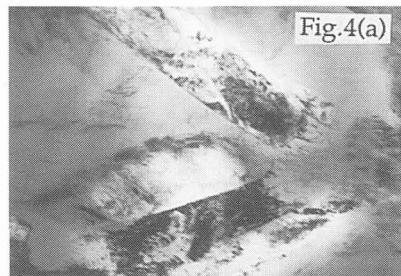


Fig. 4 - (a) Bright field image taken from the fourth domain  $T=830^\circ\text{C}$ . A reduction of the  $\alpha$  lamellae density was observed. (b) SAD pattern showing the Burgers orientation relationships. Mag. 73000X.

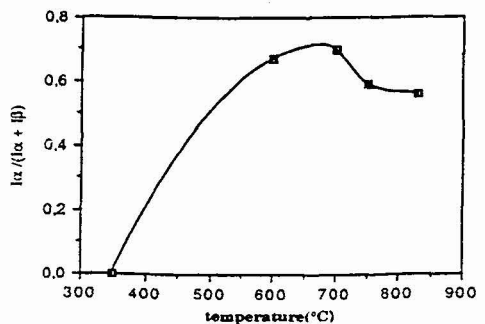


Fig. 5 - Ratio of X-ray intensities between  $\alpha$  phase and the total  $\alpha+\beta$  phases.